© 2015. Published by The Company of Biologists Ltd | Development (2015) 142, 3561-3570 doi:10.1242/dev.123281

RESEARCH ARTICLE

Allorecognition, via TgrB1 and TgrC1, mediates the transition from unicellularity to multicellularity in the social amoeba *Dictyostelium discoideum*

Shigenori Hirose[1], Balaji Santhanam[2,3], Mariko Katoh-Kurosawa[2], Gad Shaulsky[2,3,*] and Adam Kuspa[1,2,*]

ABSTRACT

The social amoeba *Dictyostelium discoideum* integrates into a multicellular organism when individual starving cells aggregate and form a mound. The cells then integrate into defined tissues and develop into a fruiting body that consists of a stalk and spores. Aggregation is initially orchestrated by waves of extracellular cyclic adenosine monophosphate (cAMP), and previous theory suggested that cAMP and other field-wide diffusible signals mediate tissue integration and terminal differentiation as well. Cooperation between cells depends on an allorecognition system comprising the polymorphic adhesion proteins TgrB1 and TgrC1. Binding between compatible TgrB1 and TgrC1 variants ensures that non-matching cells segregate into distinct aggregates prior to terminal development. Here, we have embedded a small number of cells with incompatible allotypes within fields of developing cells with compatible allotypes. We found that compatibility of the allotype encoded by the *tgrB1* and *tgrC1* genes is required for tissue integration, as manifested in cell polarization, coordinated movement and differentiation into prestalk and prespore cells. Our results show that the molecules that mediate allorecognition in *D. discoideum* also control the integration of individual cells into a unified developing organism, and this acts as a gating step for multicellularity.

KEY WORDS: Development, Self-/non-self-recognition, Social amoebae

INTRODUCTION

As cells cooperate to form organisms they must coordinate their migration, establish polarity and form specific shapes and boundaries as they integrate into different tissues during development. This process requires selective coordination of cells within a population that share physiological properties and a common environment. Such coordination is provided by soluble and cell-surface signals, but a systems-level understanding of these organizing functions is fragmentary. The social amoebae provide a model for understanding the establishment of cell cooperation during development. They behave as solitary amoebae if they have sufficient food bacteria, but undergo development when starved and form fruiting bodies with environmentally resistant spores on top of a supporting stalk (Kessin, 2001). As *D. discoideum* cells aggregate into a mound, initially as individual cells and later as streams of mutually adhesive cells, their motion is coordinated by the pulsatile secretion of a cyclic adenosine monophosphate (cAMP) signal that is relayed in spiral waves to the periphery (Tomchik and Devreotes, 1981; Kessin, 2001). Mound formation marks the first instance of the coalescence of cells into a single tissue, so it is a crucial event in the establishment of multicellularity. A key question remains regarding the mechanism by which soluble signals, such as cAMP, and cell-surface cues transmitted through adhesion proteins selectively coordinate the collection of individual cells in the mound to act as a part of an integrated organism.

We have described an allorecognition system that promotes the cooperation of cells with close relatives during multicellular development (Ostrowski et al., 2008; Benabentos et al., 2009; Hirose et al., 2011; Ho et al., 2013). The allorecognition proteins TgrB1 and TgrC1 are polymorphic in natural populations and mediate heterotypic cell-cell adhesion (Wang et al., 2000; Benabentos et al., 2009; Chen et al., 2013, 2014). Thus, the TgrB1 and TgrC1 proteins provide a possible mechanism for the cooperation that has been described in this system (Buss, 1982; Mehdiabadi et al., 2006; Gilbert et al., 2007; Ostrowski et al., 2008). We have demonstrated a role of TgrB1/TgrC1-mediated allorecognition in this process by constructing double-gene-replacement strains in the common laboratory strain AX4 to produce isogenic strains with divergent *tgrB1*/*tgrC1* allele pairs. These develop normally in pure populations, but they do not cooperate in admixtures with cells that do not share the same allele pair (Hirose et al., 2011). When strains with incompatible allotypes are mixed, cells of each type stream together into admixed mounds, but then segregate into distinct organisms and develop separately (Hirose et al., 2011). Based on these findings, we proposed that allorecognition is required to maintain the mound through the transition to multicellularity and continued development. The simplest interpretation of TgrB1/TgrC1 function would be that they act as heterophilic cell-adhesion proteins with different affinities, generating different adhesive forces for different allotype pairs, but TgrC1 also influences cAMP signaling and gene expression (Sukumaran et al., 1998; Iranfar et al., 2006), and this suggests additional roles for allotype-dependent cell communication in development.

Previous work has focused on allorecognition at the organismic level and how the segregation of mixed allotypes results in the formation of distinct organisms to allow continued development of homogeneous tissue types. Here, we define potential cellular mechanisms that depend on allorecognition and show that TgrB1 and TgrC1 regulate every function that we examined involving the integration of individual cells into a unified organism. When a minority of cells are embedded into a field of amoebae with an incompatible allotype, they are impaired in functions that are crucial

[1]Verna and Marrs McLean Department of Biochemistry and Molecular Biology, Baylor College of Medicine, Houston, TX 77030, USA. [2]Department of Molecular and Human Genetics, Baylor College of Medicine, Houston, TX 77030, USA. [3]Structural and Computational Biology and Molecular Biophysics Program, Baylor College of Medicine, Houston, TX 77030, USA.

*Author for correspondence (akuspa@bcm.edu; gadi@bcm.edu)

Received 13 February 2015; Accepted 27 August 2015

Development (2015) 142, 3561-3570 doi:10.1242/dev.123281

for the integration of individual amoebae into the newly forming multicellular organism. Cell polarization for directional movement, coordinated movement with other cells and cell differentiation do not occur when the minority allotype cells are isolated, but these functions are restored when the cells encounter other cells with the same allotype. Our findings suggest that allorecognition is an essential mediator of the transition from the unicellular state to the multicellular state.

RESULTS

Allorecognition is an active recognition process

The patterns of segregation observed when cells of incompatible allotypes are mixed suggested that cells might actively recognize and/or reject non-self individuals (Hirose et al., 2011). To characterize further the process of allorecognition, we carried out transcriptome analyses of cell mixtures during the acquisition of multicellularity. Five isogenic *tgrB1-tgrC1* gene replacement strains with mutually incompatible allotypes were mixed and allowed to co-develop (referred to here as the 5-way mixture). An amoeba would have an ∼80% chance of interacting with incompatible allotypes, ensuring a high level of non-self encounters prior to the time when each of the five allotypes coalesce into distinct regions of the aggregate after mound formation and develop as segregated homogeneous populations. We compared the RNA isolated from this mixture with a reference mixture of RNA samples of the same five strains developed as pure populations. We collected RNA samples before (4 h), during (8 h) and after (12 h) the onset of allorecognition, analyzed them by RNA-seq, and compared transcript abundances between the 5-way mixture and the mixed pure population samples. The results are shown as a plot that describes the fold difference in RNA abundance for each transcript and the confidence of the measurement (Fig. 1) and in tabular form in Table S1. No genes showed significant differences in expression at 4 h of development, indicating that development proceeded in the same way in the mixture as it did in the pure populations up to this time (Fig. 1; Table 1). At 8 h, 68 genes displayed significantly different expression in the 5-way mixture compared with the pure populations, and at 12 h 85 genes showed altered expression. Only one gene showed altered expression at both 8 and 12 h, suggesting that most changes were transient.

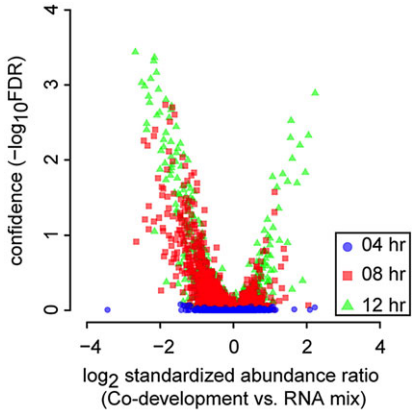

Fig. 1. Transcriptional response to allotype incompatibility. The mRNA abundances at 4, 8 and 12 h are plotted for five strains with mutually incompatible allotypes that were allowed to co-develop, and compared with a control RNA sample made from the five strains developed separately. We compared mRNA abundance between the co-developed and the mixed RNA (RNA mix) samples by RNA-seq (Materials and Methods; Table S1). The result is shown as the confidence ($-\log_{10}$ of the false discovery rate) versus the fold difference in normalized read counts. Symbols represent individual genes at each time of development; 4 h (blue), 8 h (red) and 12 h (green).

Table 1. Differential gene expression in developing allotype admixtures

Time (h)	Higher expression genes*	Lower expression genes‡	Total
4	0	0	0
8	2	66	68
12	14	71	85
Total	16	136§	152§

*,‡The number of genes that displayed a >twofold higher (*) and lower (‡) normalized read count with confidence >1.0 are shown.
§One gene (DDB_G0280717) displayed lower expression at both 8 and 12 h.

Eight hours is the time that cells begin to integrate into the mound and when we would predict a response to self or to non-self would be reflected in the combined transcriptomes of the mixed allotypes as strains with different allotypes segregate into distinct aggregates starting at this time (Hirose et al., 2011). The observation that 16 genes that are expressed at higher levels in the 5-way mixtures suggests that the cells are actively responding to non-self (Table 1; Table S2). The lower expression of 66 genes that are normally expressed at 8 h of development indicates a delay in the transcriptional program in the 5-way mixture because all but one of those genes are expressed normally by 12 h (Table 1; Table S2; Fig. S1). One interpretation of this delay is that the cells do not progress normally because they fail to detect cells of the same allotype. The observation that 71 genes displayed lower expression at 12 h in the 5-way mixture is consistent with this idea (Table 1; Table S2). A Gene Ontology (GO) enrichment analysis revealed an over-representation of extracellular matrix protein genes in this group (Table S3). The Tgr genes also appear to be over-represented. There are 37 Tgr genes out of the 12,869 genes that we measured and six of these are among the 152 genes displaying altered expression (odds ratio 16.7, $P=4.4\times10^{-6}$; Fisher's exact test). These data support an active process of allorecognition because we find 152 differentially expressed genes when multicellularity is being established, and no expression differences at 4 h, while the cells are behaving as individuals.

Allorecognition is required for coordinated cell movement as multicellularity is established

To examine the allorecognition response at the single-cell level, we followed individual fluorescently labeled cells during mound formation when mixed at low proportions with unlabeled cells of compatible, or incompatible, allotypes (Fig. 2A). We analyzed the displacement and the change in direction (variance of angle) for individual cells. Each panel in Fig. 2B is rendered as a composite of 15 successive images of cells labeled with green or red fluorescent protein (GFP or RFP, respectively), so that individual cell tracks are apparent. Cells that were compatible with the majority of unlabeled cells (RFP, in red) displayed consistent radial movement, whereas the incompatible cells (GFP, in green) moved discontinuously and turned more frequently (Fig. 2B; Movie 1). We also observed a large number of incompatible cells that moved to the periphery and out of the aggregate altogether.

We confirmed our observations of cell movement over many repetitions of this type of experiment using different allotype combinations and through the quantification of the movement of individual cells (Fig. 2C-E). The mean displacement of cells increased during the first 6 h of the experiment (corresponding to 6-11 h after starvation) and reached a steady maximum level

Development (2015) 142, 3561-3570 doi:10.1242/dev.123281

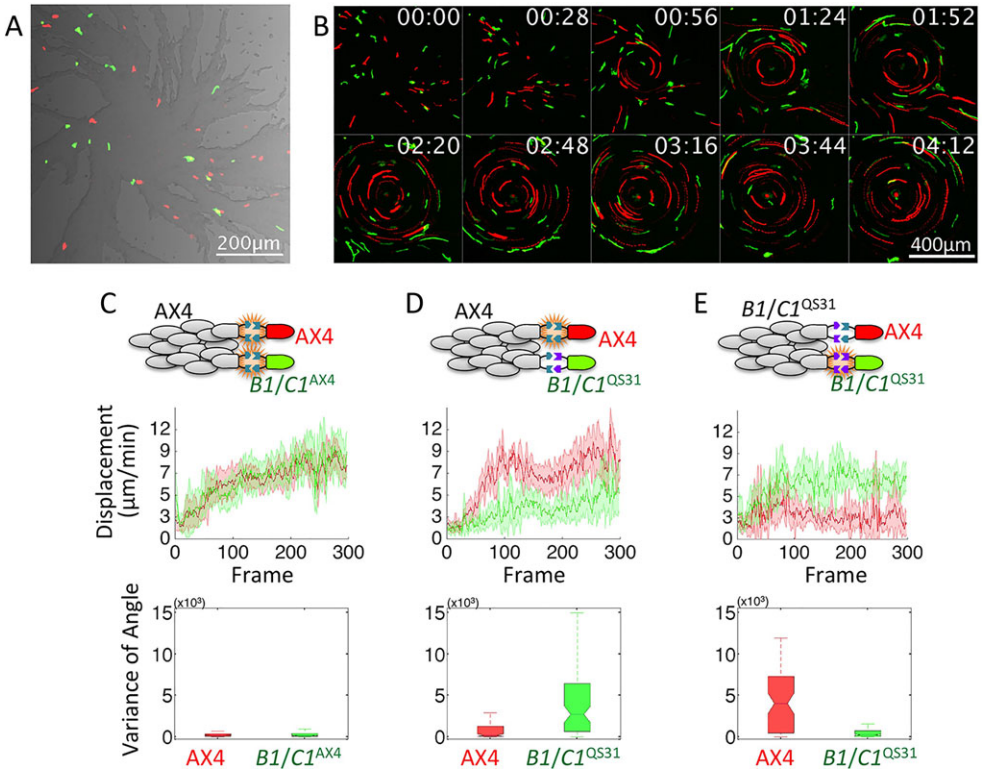

Fig. 2. Coordinated movement during aggregation requires allorecognition. (A) A representative image of an unlabeled majority strain (99.6%) mixed with GFP- or RFP-labeled minority strains (0.2% each), with compatible or incompatible allotypes. (B) Panels showing the migration trajectories of compatible (red), and incompatible (green) cells (15 consecutive frames overlaid in a single image, 1 frame/min) with 28-frame interval (time is in hours and minutes). (C-E) Quantified migration of GFP and RFP cells. The color-coded diagrams show the strain combination of majority (gray), GFP-labeled (green) and RFP-labeled (red) cells with different TgrB1/TgrC1 allotypes. Cell positions were recorded every minute for 5 h, after 6 h of starvation. The upper graphs show the frame-to-frame mean displacement (±standard error) of every cell in the frame. The box plots (lower panels) show the summary of the change in their direction of movement for all GFP/RFP cells. The color of each plot corresponds to the strain labeled with GFP (green) or RFP (red). (C) Strains with identical *tgrB1* and *tgrC1* alleles; AX4, 0.2% of AX4-RFP, and 0.2% $tgrB1^{AX4}tgrC1^{AX4}$-GFP ('$B1/C1^{AX4}$'). (D) The GFP-labeled $tgrB1^{QS31}tgrC1^{QS31}$ strain is incompatible with the AX4 majority and the AX4-RFP cells. (E) Reciprocal of the data shown in D, with $tgrB1^{QS31}tgrC1^{QS31}$ as the majority allotype, with 0.2% AX4-RFP cells and 0.2% $tgrB1^{QS31}tgrC1^{QS31}$-GFP cells.

thereafter, as previously reported (Rietdorf et al., 1996). Surprisingly, we found that the movement of incompatible cells was compromised, as indicated by the reduced mean displacement of the cells and their increased turning, which determined the change in their direction of movement (Fig. 2C-E). The compatible strain that we used as a control had its original $tgrB1^{AX4}/tgrC1^{AX4}$ alleles replaced with the same $tgrB1^{AX4}/tgrC1^{AX4}$ alleles and this strain behaved indistinguishably from the parental AX4 cells (Fig. 2C), so the genetic manipulations used for allele replacement did not affect the process. In the first experiment, the compatible cells (red) moved normally, whereas the incompatible cells ($tgrB1^{QS31}tgrC1^{QS31}$, green), that have the $tgrB1^{QS31}/tgrC1^{QS31}$ alleles instead of $tgrB1^{AX4}/tgrC1^{AX4}$ alleles, displayed reduced displacement and increased turning (Fig. 2D). In the reciprocal mixture, the now compatible $tgrB1^{QS31}tgrC1^{QS31}$ cells (green) behaved normally when mixed with a majority of compatible unlabeled $tgrB1^{QS31}tgrC1^{QS31}$ cells, whereas the labeled AX4 cells (red) displayed aberrant movement in the same mounds (Fig. 2E). We confirmed the statistical significance of the differences in displacement between the populations of compatible versus incompatible cells using the Kolmogorov-Smirnov test (Fig. S2). These observations were consistent through several repetitions and suggest that a compatible allotype is required for the coordinated movement of cells during mound formation, but is not required for earlier steps in aggregation because the individual minority cells were able to enter the aggregate regardless of their allotype. The reciprocal mixing combinations in Fig. 2D,E indicate that the results were only affected by the allotype compatibility, not by the experimental choice of allotypes. The impaired movement of individual incompatible cells must also be independent of soluble signals because they are exposed to the same environment as the other cells in the mound. Our ability to examine the behavior of a single incompatible cell and show that it does not engage in coordinated cell movement with the surrounding non-self cells suggests that the normal radial cell movement during mound formation crucially depends on active allorecognition.

A possible interpretation of these findings was that the allorecognition system inhibits development in a cell that only encounters cells with incompatible allotypes. We tested this possibility by using AX4 strains that carry an additional pair of Tgr genes ($tgrB1^{QS4}tgrC1^{QS4}$ or $tgrB1^{QS31}tgrC1^{QS31}$). When these merodiploid cells were in the majority, any minority cell with a compatible pair of Tgr genes moved in a coordinated manner with them (Fig. 3A,B; Fig. S2). When the merodiploid cells were in the minority, they also moved in a coordinated manner as long as one of their two pairs of Tgr genes was compatible with the majority allotype in the mixture. An example of this is shown in Fig. 3 for the merodiploid containing Ax4 and QS31 Tgr allele pairs, mixed together as a minority of cells with the two compatible allotypes as the majority and with one incompatible allotype (Fig. 3C-E;

Development (2015) 142, 3561-3570 doi:10.1242/dev.123281

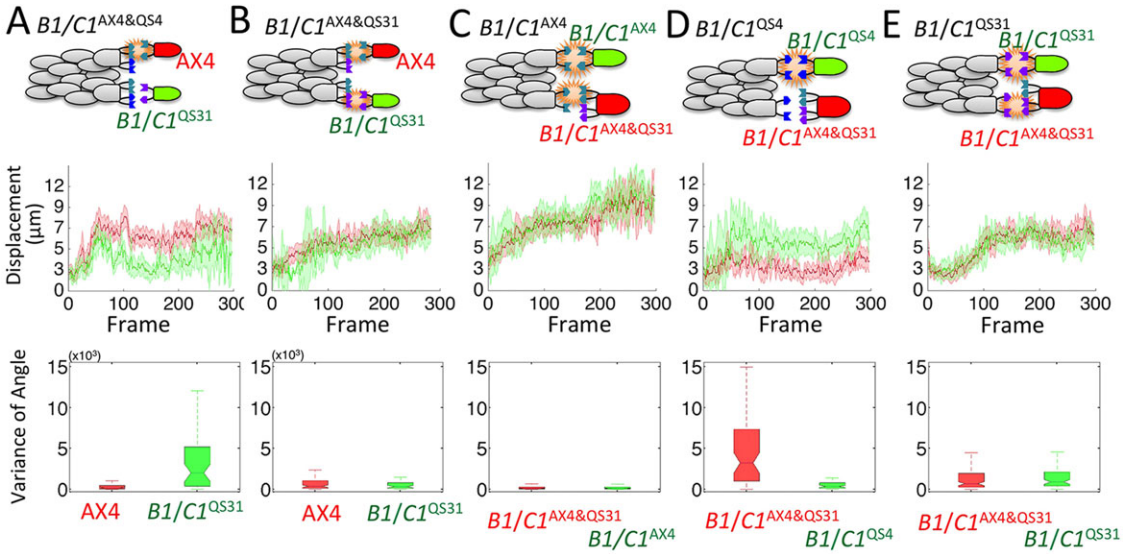

Fig. 3. Migration of cells with two *tgrB1/tgrC1* allele pairs specifying distinct allotypes. Quantified cellular movement as described in Fig. 2. The upper panels show diagrams of the strain combinations as in Fig. 2C,E, the middle panels show the frame-to-frame mean displacement (±standard error) of every labeled cell in the frame, and the lower panels show the change in their direction. (A,B) Merodiploids (AX4 carrying an extra *tgrB1/tgrC1* allele pair from strains QS4 or QS31) were used as the majority cells and labeled cells were either compatible with one of the two pairs, or incompatible with both pairs. (C) AX4 mixed with AX4-GFP and the merodiploid *tgrB1*^{AX4}*tgrC1*^{AX4}, *tgrB1*^{QS31}*tgrC1*^{QS31}-RFP ('*B1/C1*$^{AX4\&QS31}$'). (D) Unlabeled *tgrB1*^{QS4}*tgrC1*^{QS4} majority mixed with *tgrB1*^{QS4}*tgrC1*^{QS4}-GFP and a *tgrB1*^{AX4}*tgrC1*^{AX4}, *tgrB1*^{QS31}*tgrC1*^{QS31}-RFP merodiploid. (E) Unlabeled *tgrB1*^{QS31}*tgrC1*^{QS31} majority mixed with *tgrB1*^{QS31}*tgrC1*^{QS31}-GFP and a *tgrB1*^{AX4}*tgrC1*^{AX4}, *tgrB1*^{QS31}*tgrC1*^{QS31}-RFP merodiploid.

Fig. S2). We did not detect negative effects on cell movement in cells expressing an extra pair of non-matching Tgr proteins, indicating that the mechanism of allorecognition is inclusive and excitatory rather than inhibitory.

Allorecognition is required for cell polarization and cAMP sensing

Given that our experiments suggested that coordinated cell movement requires self-recognition, we examined cell polarization and cAMP sensing in compatible and incompatible cells during mound formation. We examined cell polarization using a probe that localizes to the posterior of migrating cells, the actin-binding domain (ABD) of ABP-120 (filamin) fused to GFP (Pang et al., 1998; Washington and Knecht, 2008). Persistently migrating cells expressing GFP-ABD displayed stable posterior GFP localization, demonstrating that the cells are polarized. When ABD-GFP cells were mixed with a majority of compatible cells, they moved persistently with polarized posterior localization of GFP (Fig. 4A-E; Movie 2). The same cells failed to polarize or move properly when mixed with a majority of incompatible cells (Fig. 4F-J; Movie 2). We quantified cell polarization by examining the GFP signal at the cell perimeter. Sample kymographs showed stable posterior localization of GFP when the cells were mixed with a majority of compatible cells (Fig. 4D), but not when they were mixed with an incompatible allotype (Fig. 4I), confirming the previous result where incompatible cells failed to migrate coordinately and persistently (Fig. 2D-E; Fig. 4J). These experiments suggest that sustained polarization of individual cells during mound formation requires allorecognition.

Previous studies have also suggested that cooperative cell movement in the mound is coordinated by spiral waves of diffusible cAMP (Weijer, 2009). Therefore, we also examined cell polarization during mound formation as revealed by the cAMP-responsive protein fusion PH-GFP. The pleckstrin homology (PH) domain in PH-GFP derives from CRAC (cytosolic regulator of adenylyl cyclase), a protein that localizes to the anterior cortex of migrating cells in response to extracellular cAMP (Parent et al., 1998). In control experiments in which all of the cells expressed PH-GFP, we observed coordinated waves of anterior GFP localization with roughly 6-min periodicity (data not shown). To examine the role of allorecognition in cAMP responsiveness, we embedded AX4 cells that were co-expressing PH-GFP and RFP, AX4RFP[*PH-GFP*], along with *tgrB1*^{QS31}*tgrC1*^{QS31} cells expressing *PH-GFP*, *tgrB1*^{QS31}*tgrC1*^{QS31}[*PH-GFP*], within a majority of unlabeled AX4 cells. This enabled us to observe the differential responses of distinct allotypes to cAMP within the same aggregate. In one example of many such experiments shown in Fig. 5 and Movie 3, PH-GFP localized normally to the compatible cells' anterior, but failed to localize in the incompatible cell (Fig. 5A-F; Movie 3), as shown in the kymographs depicting GFP localization at the cell perimeter (Fig. 5G,H). Consistent with our findings described above (Fig. 4), the movement of the compatible cell was persistent and coordinated with the majority of cells, whereas the incompatible cell lagged (Fig. 5I,J). Additional examples of this are shown in Fig. S3.

The failure of PH-GFP to localize to the cell anterior of incompatible cells could be because of a general defect in cAMP responsiveness. Therefore, we tested the chemotactic properties of the cells taken directly from the admixed mounds. Separately, we pulsed admixed cells with cAMP in shaken suspensions in which cell-cell contact is substantially limited by hydrodynamic shear forces. We found no differences in the displacement or chemotactic index between cells of the compatible or incompatible minority allotypes, demonstrating that the cells are not generally defective in chemotaxis when tested as individual cells, and that incompatible cells have the same chemotactic potential as the compatible cells (Fig. S4). Together, these results suggest that the proper polarization of cells during mound formation, and their responsiveness to cAMP, require contact with other cells of the same allotype. Unexpectedly,

Development (2015) 142, 3561-3570 doi:10.1242/dev.123281

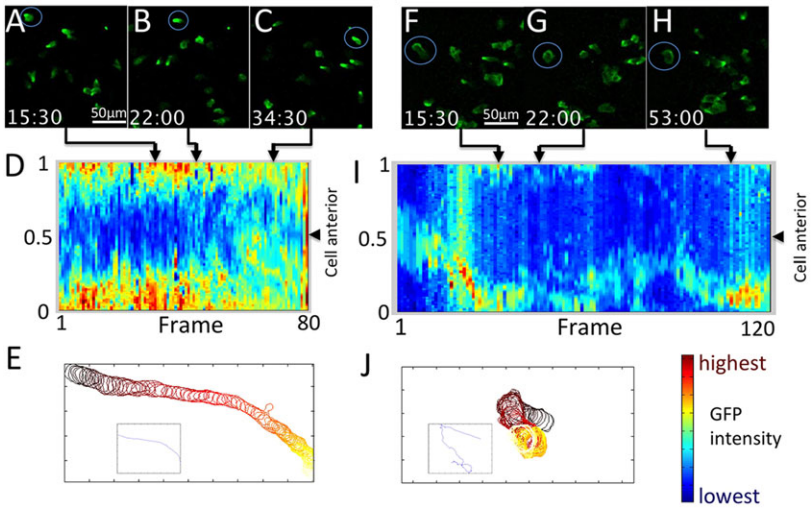

Fig. 4. Allotype compatibility is required for cell polarization. (A-J) Images showing AX4 cells expressing GFP-fused ABD (AX4[*GFP-ABD*]) mixed with *tgrB1*^{AX4}*tgrC1*^{AX4} (A-E; Movie 2; time in minutes and seconds), or *tgrB1*^{QS31}*tgrC1*^{QS31} (F-J; Movie 2). The majority cells (unlabeled) are not observable here, but can be seen in bright-field images in Movie 2. (A-C) One percent of AX4[*GFP-ABD*] cells were mixed with 99% unlabeled *tgrB1*^{AX4}*tgrC1*^{AX4} cells. (D) The polarity of one cell (circled in A-C) is shown as a kymograph of GFP boundary fluorescence with QuimP software (Bosgraaf and Van Haastert, 2010). The *y*-axis is the normalized boundary of the cell, with 0 and 1 as the posterior and 0.5 as the anterior. The one-dimensional data are concatenated frames along the *x*-axis and the arrows connect images with the corresponding position in the kymograph. (E) The cell outlines in every frame were identified using QuimP software and overlaid in a single image. The brown to yellow gradient indicates the passage of time. The inset shows the centroids of the cell in every image connected by a line. (F-J) One percent of AX4[*GFP-ABD*] cells were mixed with 99% unlabeled incompatible *tgrB1*^{QS31}*tgrC1*^{QS31} cells. In this typical example, the localization of GFP-ABD in the circled cell (F-H) shows no stable pattern (I) and the cell translocates little in these frames with an erratic migration trajectory (J).

we also found that cells isolated from mounds displayed significantly reduced responsiveness to cAMP (Fig. S4).

Allorecognition triggers cell polarization and cooperative cell movement

One explanation for the uncoordinated movement of incompatible cells could be that sustained TgrB1/TgrC1 signaling is needed for cells to acquire the capacity for coordinated behavior. Minority cells occasionally encountered one another in the mound and those events allowed us to examine this possibility. We followed the circled cell in Fig. 4F for an hour while it was surrounded by incompatible cells and non-polarized. This cell then entered into a clump of compatible cells and within 10 min began migrating in a circular pattern with the group (Fig. 6A-D; Movie 2). All the cells in the rotating clump appeared to polarize at the same time, as indicated by the coordinated localization of the ABD-GFP signal (Movie 2). The spinning behavior of minority cell clumps is seen in every experiment, but not all clumps display the behavior (e.g. the clump below the spinning clump in Movie 2). Thus, minority incompatible cells are indeed capable of coordinated cell movement and contact with cells of a matching allotype can induce an immediate change in cell behavior.

To examine cell polarity within spinning minority clumps, we labeled the nuclei of the minority cell subpopulation with RFP-H2b (histone 2B fused to monomeric RFP; Fischer et al., 2004) and additional minority cells of the same allotype with ABD-GFP. We embedded both strains within a majority of incompatible cells and followed their development. The more abundant RFP nuclear signals allowed us to detect the occasional clumps of the minority incompatible cells and the ABD-GFP signals allowed us to monitor

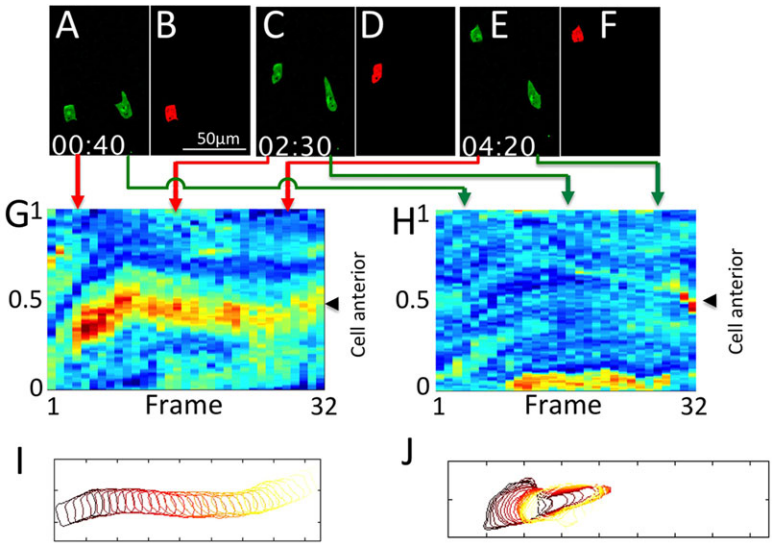

Fig. 5. Allotype compatibility is required for cAMP responsiveness. PH-GFP localizes to the anterior of cells responding to extracellular waves of cAMP signal and we use this as a measure of cAMP responsiveness in cells with compatible and incompatible allotypes within the same aggregate. (A-F) AX4 cells co-expressing PH-GFP and RFP (AX4RFP[*PH-GFP*]) and *tgrB1*^{QS31}*tgrC1*^{QS31} cells expressing PH-GFP (*tgrB1*^{QS31}*tgrC1*^{QS31}[*PH-GFP*]) were embedded in a majority (98%) of unlabeled AX4 cells. Green fluorescence images (A,C,E) and red fluorescence images (B,D,F) of three time points are shown. (G) Typical kymograph of PH-GFP localization in AX4RFP [*PH-GFP*] while migrating in a field of AX4 cells, displays strong GFP localization at the leading edge (position 0.5). The red arrows indicate the corresponding frames. (H) Kymograph of PH-GFP localization in *tgrB1*^{QS31}*tgrC1*^{QS31}[*PH-GFP*] displaying no significant accumulation of GFP signal at the leading edge. The signal near position 0 comes from the nucleus (Movie 3). The green arrows indicate the corresponding frames. (I) The trajectory of the AX4*RFP*[*PH-GFP*] cell for every frame in G. (J) The migration trajectory of *tgrB1*^{QS31}*tgrC1*^{QS31} [*PH-GFP*] for every frame in H. The brown to yellow gradient indicates the passage of time.

Development (2015) 142, 3561-3570 doi:10.1242/dev.123281

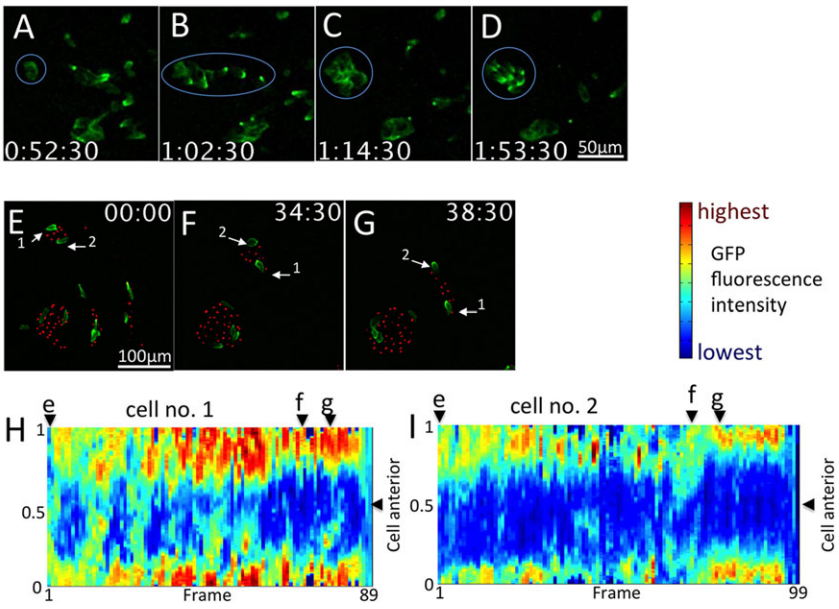

Fig. 6. Allorecognition triggers cell polarization and cooperative movement. (A-D) Time series of AX4[GFP-ABD] embedded in a majority of *tgrB1*^{QS31}*tgrC1*^{QS31} cells, continuing the experiment shown in Fig. 4F-J. The circled cell in A is identical to the cell in Fig. 4F-H. The singleton in A was surrounded by incompatible AX4 and did not display persistent polarity (Fig. 4I). This cell formed a clump with cells of the same allotype (B,C) and displayed coordinated cell movement (Movie 2) and persistent cell polarity (D). (E-G) To visualize single-cell polarity within a clump, 1% AX4[RFP-H2b] and 0.05% AX4[ABD-GFP] were embedded in the majority of *tgrB1*^{QS31}*tgrC1*^{QS31}. The two differentially labeled AX4 cells cooperate in circular migration within the majority of incompatible cells (also see Movie 4). (H,I) Kymographs of the two cells in E-G show that their polarity is similar to cells embedded in the same allotype in Fig. 4D. Letters (e-g) indicate the frames that correspond to the panels above.

the polarization of individual cells within the clumps. When non-polarized minority cells came together and formed small clumps within the field of the majority incompatible cells they began to coordinate their movement as indicated by the direction and speed of the red-labeled nuclei, and became polarized in the clump as indicated by the few ABD-GFP-labeled cells (Fig. 6E-G; Movie 4). Kymographs of GFP fluorescence intensity at the cells' perimeter provided quantitative evidence for cell polarization (Fig. 6H,I). These results demonstrate that coordinated migration of polarized cells is triggered by contact with compatible cells.

Allorecognition is required for cell differentiation

As the amoebae complete their integration into a multicellular organism, distinct populations of cells begin to express sets of genes that define the presumptive tissues. The *cotB* gene encodes a spore coat protein and its activation has been used extensively as a marker for prespore cell differentiation (Williams, 1997). To examine the potential role of allorecognition, we placed a gene encoding GFP under the control of the *cotB* promoter (*cotB*/*GFP*) and introduced the construct into our test cells, along with the constitutively expressed RFP to identify marked cells. We embedded a minority of the AX4RFP[*cotB*/*GFP*] test cells within a majority of cells with either a compatible allotype (AX4) or an incompatible allotype (*tgrB1*^{QS31}*tgrC1*^{QS31}) and visualized prespore differentiation by expression of GFP. When the marked test cells were present at 1% they expressed *cotB/GFP* when surrounded by cells of the same allotype (Fig. 7A), but not when surrounded by incompatible cells (Fig. 7B). When we increased the proportion of minority allotype cells to 5% they expressed the *cotB*/*GFP* as single cells among the compatible majority and when they were mixed with an incompatible majority they clumped together and expressed *cotB*/*GFP* (Fig. 7C,D). This demonstrates that the cell-type marker was functional and that the minority cells are capable of differentiation, as long as they interact with compatible cells.

We quantified these observations of *cotB* expression by measuring the population distribution of GFP expression by flow cytometry. We replaced GFP with a fast-folding variant of GFP (sfGFP) to improve our ability to detect *cotB* expression sooner after promoter activation. When incompatible cells were present as a 1% minority, they expressed little or no *cotB*/*sfGFP*, whereas most of the cells expressed normal levels when those same cells were developing with compatible cells (Fig. 7E). As shown in Fig. 7D, *cotB* was expressed normally when those same cells were present as 5% of the mixture and clumped together within the mound (Fig. 7F). We obtained similar results with two other prespore gene reporters, *pspA/sfGFP* and *pspD/sfGFP* (Fig. S5), suggesting that allorecognition is required for prespore differentiation. The extracellular matrix protein encoded by *ecmA* is broadly expressed in the prestalk cell lineages that make up ~20% of the cells in the developing mound (Williams, 1997). We followed its expression using *ecmA/sfGFP* using the same experimental approach that we used to follow prespore gene expression (Fig. 7G,H). As with the prespore gene expression, when incompatible cells were present as a 1% minority, they expressed little or no *ecmA*/*sfGFP*, and most of the cells expressed the higher level observed when those same cells were developing with compatible cells (Fig. 7G). These results suggest that allorecognition is important for the differentiation of both prestalk and prespore cells. Conversely, the initial expression of the *tgrB1* and *tgrC1* genes, which begins several hours prior to cell differentiation, is independent of allorecognition (Fig. S6).

We next tested whether cell differentiation requires sustained cell contact between compatible allotypes. We mixed minority allotype cells carrying *cotB*/*sfGFP* at various ratios with compatible or incompatible cells and quantified prespore gene expression. In the control mixtures with a compatible allotype majority, the minority marked cells expressed *cotB* with the same population distribution (Fig. 8A). However, when the minority *cotB*/*sfGFP* cells were mixed with a majority of incompatible cells, we observed what appears to be an 'all-or-nothing' expression in the minority cell population. At levels of 0.2% and at 1% the minority cells displayed a similar population distribution of poor *cotB* expression, but at 5% and 20% the cells displayed a similar distribution to the mixture with compatible majority (Fig. 8B). Minority cells that were mixed at 5% and 20% clumped together and formed regions of minority allotype tissue within the mound, as seen in Fig. 7D (full data set not shown). We obtained similar results for two other prespore genes, *pspA* and *pspD* (Fig. S7A-D).

Development (2015) 142, 3561-3570 doi:10.1242/dev.123281

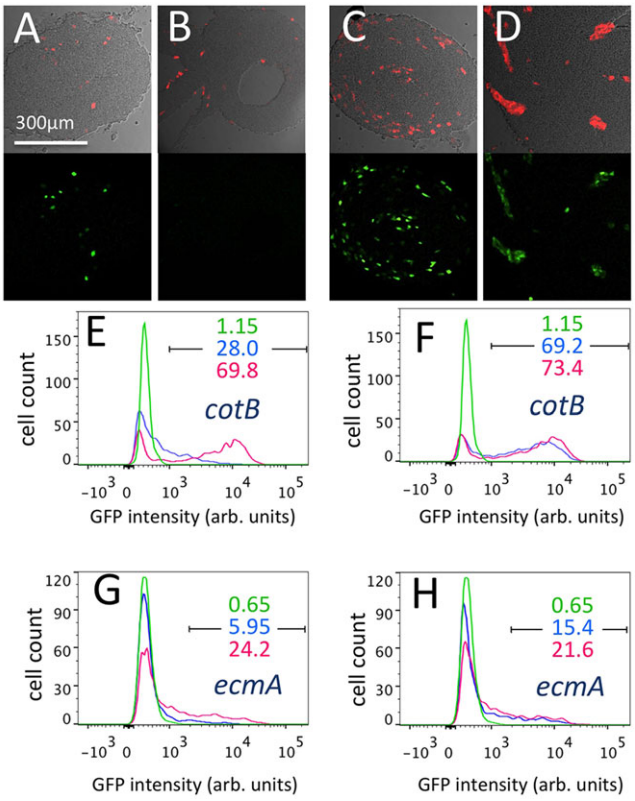

Fig. 7. Role for allotype recognition in cell differentiation. (A-D) Bright-field images overlaid with fluorescence images (upper panel), and the GFP expression in those cells (bottom panel) showing the location of AX4RFP[*cotB*/*GFP*] cells (1%) embedded within AX4 cells (99%) (A), AX4RFP[*cotB*/*GFP*] cells (1%) embedded within *tgrB1*^{QS31}*tgrC1*^{QS31}cells (99%) (B), AX4RFP [*cotB*/*GFP*] cells (5%) embedded in AX4 cells (95%) (C), or *tgrB1*^{QS31}*tgrC1*^{QS31} cells (95%) (D). (E,F) *cotB* promoter activation was quantified by flow cytometry in AX4RFP[*cotB*/*sfGFP*] cells developing together with AX4, or *tgrB1*^{QS31}*tgrC1*^{QS31} cells for 10 h. The intensity of green fluorescence (GFP) is plotted for the RFP-positive cell population. The green plot shows growing AX4RFP[*cotB*/*sfGFP*] cells before development. Minority AX4RFP[*cotB*/*sfGFP*] cells were 1% (E) or 5% (F) of the cells in mixtures with incompatible *tgrB1*^{QS31}*tgrC1*^{QS31} cells (blue plots) or compatible AX4 cells (red plots). The colored numbers indicate percentages of cells within the window of the respective colored plot (set to be identical in panels E and F). (G,H) The expression of a prestalk gene, *ecmA*, was examined as above after 16 h of development. The green plot shows growing AX4RFP[*ecmA*/*sfGFP*] cells before development. Minority AX4RFP[*ecmA*/*sfGFP*] cells were 1% (G) or 5% (H) of the cells in mixtures with incompatible *tgrB1*^{QS31}/*tgrC1*^{QS31} cells (blue plots), or compatible AX4 cells (red plots).

The induction of cell-specific gene expression can occur in low-cell-density monolayers of starving cells, without the formation of aggregates or other obvious developmental morphogenesis. Such systems have been used for decades to study the signaling requirements for prespore, or prestalk, cell differentiation (Williams, 1997; Thompson and Kay, 2000). Our results predict that a critical density of cells would be required for *cotB* expression in low cell-density monolayers that would allow for cell-cell contact. We tested this in our system with pure populations of *cotB*/sfGFP marked cells. At densities of 5×10^4 cells/cm^2 and 5×10^5 cells/cm^2, the cells that were in contact with other cells in clumps expressed *cotB*, but at 5×10^3 cells/cm^2 the cells were clearly separated and no cells expressed *cotB* (Fig. 8C). We obtained similar results with another prespore gene, *pspD* (Fig. S7E). Taken together, these results suggest that cell differentiation requires contact between cells that share the same allotype, even in cell suspensions.

DISCUSSION

Intraspecific chimerism is seen in bacteria and unicellular eukaryotes for which self-recognition is a significant component of the establishment or maintenance of multicellular interactions, even in seemingly 'clonal' organisms (Buss, 1982). A number of allorecognition and patterning systems in animals, in which cells are clonal by definition, also rely on polymorphic membrane proteins with immunoglobulin-like folds, as found in TgrB1 and TgrC1 (Hughes and Nei, 1988; Boehm, 2006; Hattori et al., 2007; Matthews et al., 2007; Rosa et al., 2010). We have demonstrated that TgrB1 and TgrC1 are allorecognition components in *D. discoideum* and that they can promote cooperation on an organismic level by preventing exploitation by strains with incompatible allotypes (Benabentos et al., 2009; Hirose et al., 2011; Ho et al., 2013). Here, we have shown that allorecognition between amoebae that share compatible TgrB1 and TgrC1 variants leads to cellular cooperation that is essential for multicellular development. Coordinated cell movement, cell polarization and cell differentiation each appear to require the engagement of TgrB1 and TgrC1 between cells. This does not seem to occur passively through cell adhesion alone, because contact between incompatible allotypes significantly alters their transcriptional program and that contact between compatible allotypes results in immediate changes in the behavior of the amoebae. Thus, we propose that allorecognition and the establishment multicellularity are coupled by active signaling through TgrB1 and TgrC1.

Individual cells do not polarize when their allotype is incompatible with surrounding cells in the mound, as we observed using stable GFP-protein fusions that mark the anterior or posterior of polarized cells. This is a striking finding in that these singleton cells are exposed to the same field-wide soluble signals as the other cells in the mound yet they do not polarize and do not move coordinately with the group. Our observation that the PH-GFP protein does not localize to the anterior of singleton cells indicates that their response to cAMP is impaired. Given that cell polarization and coordinated movement are activated immediately after those same cells encounter other cells with a compatible allotype, allorecognition appears to be reinforced, at least in part, by stimulation of cooperative motility.

It is notable that both compatible and incompatible cells, tested as isolated cells, became significantly less responsive to cAMP gradients during the transition from streaming aggregation to mound formation compared with cells pulsed with cAMP in suspension, and the motility of the developing cells decreased over time (Fig. S4A). This finding contrasts the increase in cell motility we observed over developmental time within the mound (Fig. 2C), suggesting that cAMP chemotaxis does not govern the rate of cell movement in the mounds. The decrease in the responsiveness to cAMP of individual cells isolated from developing populations appears to be unrelated to allorecognition because both compatible and incompatible minority cells display the same decrease (Fig. S4). Furthermore, we also observed small clumps of minority allotype cells in mounds that move in 'pinwheels' and in straight lines, in a manner that is completely uncoordinated with the majority cells in which they are embedded (Movie 4). These observations are inconsistent with the regulation of cell motility by soluble cAMP signaling. So, even though signaling through the cAMP receptor cAR2 is required for development at this time (Saxe et al., 1993), the detection of cAMP signals through cAR2 does not appear to trigger the coordinated migration of cells. In addition, extracellular cAMP signaling can be bypassed in aggregation-stage adenylyl cyclase (ACA) mutants by activating PKA and those cells display

Development (2015) 142, 3561-3570 doi:10.1242/dev.123281

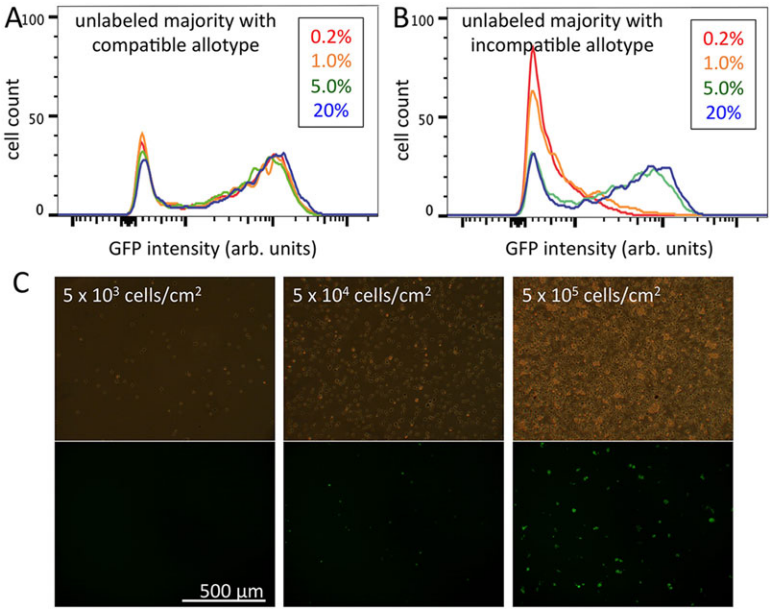

Fig. 8. Cell density requirement for cell differentiation. (A,B) *cotB* promoter activation was quantified by flow cytometry in AX4RFP[*cotB*/*sfGFP*] cells developing together with AX4 cells (A, compatible allotype) or *tgrB1*^{QS31}*tgrC1*^{QS31} cells (B, incompatible allotype) for 10 h. The intensity of green fluorescence (GFP) is plotted for the RFP-positive cell population. The inset shows the percentage of the labeled cells in the mixture for the respective colored plot. (C) A monolayer of AX4[*cotB*/*sfGFP*] cells incubated in buffer for 24 h with 5 mM cAMP, at the cell densities indicated. Shown are bright-field images of the cells (upper panels) and the corresponding fluorescent images (lower panels) revealing GFP-expressing cells.

coordinated cell movement and cell differentiation, and carry out tissue morphogenesis (Wang and Kuspa, 1997; Rappel et al., 1999). Our results are consistent with the contact-stimulated transmission of cAMP between cells that has been previously proposed (Umeda and Inouye, 2002; Kriebel et al., 2008). Alternatively, the cooperative cell movement mediated by TgrB1/TgrC1 might be independent of extracellular cAMP signaling, involving other chemical, vesicular or mechanical signaling pathways that are promoted by cell contact, as has been described for tissue morphogenesis in other systems (Weijer, 2009; Mammoto et al., 2013; Lee et al., 2014; Zhang and Wrana, 2014). If true, cAMP might still signal through cAR2, or other cAMP receptors, and act as a chemokine or in another subsequent step in the developmental program.

The movement of minority cells in single-file through a field of radially moving incompatible cells (Movie 4) also suggests that TgrB1 and TgrC1 promote end-to-end adhesion rather than lateral cell-cell adhesion. This is consistent with the report that TgrB1 and TgrC1 establish associations within the membrane of one cell that is stimulated by their interactions between cells, suggesting the formation of TgrB1/TgrC1 adhesion patches (Chen et al., 2014).

The *D. discoideum* multicellular structure consists of prestalk and prespore tissues. Some tissue-specific genes, including *ecmA* and *pspA*, are inducible in low cell-density monolayers with added cAMP and DIF (e.g. Thompson and Kay, 2000). This seems at odds with our observations that minority incompatible cells fail to induce these genes within mounds even though they were exposed to the field-wide extracellular stimuli, but do express the genes if they engage cells with a compatible allotype. However, we observed that cell differentiation markers are induced in a cell density-dependent manner using the same monolayer system and that the crucial transition is the density at which the cells are in close contact with one another. This suggests that cell contact is required for cell differentiation of strains derived from the wild strain NC4, such as AX4, even in monolayer experiments, and this is consistent with our observation that allorecognition is required *in vivo*. Serafimidis and Kay also reported a dependence of cell differentiation on cell density in NC4-derived strains (Serafimidis and Kay, 2005). However, another wild strain, V12M2, is able to form spores *in vitro* without cell contact, with added cAMP and media conditioned by starving cells for 18 h (Kay, 1982). These *in vitro* observations suggest that the development of V12M2 does not depend on TgrB1/TgrC1-mediated allorecognition, though there is no direct data to support this. This could be tested by replacing *tgrB1* and *tgrC1* in V12M2 with a variant pair of genes to test if the derivative strain co-develops with V12M2, as we did here with the NC4-derived strains and as reported previously (Hirose et al., 2011). It should be kept in mind, however, that all 29 wild strains of *D. discoideum* that we examined had highly divergent *tgrB1* and *tgrC1* genes, suggesting that allorecognition is widespread, if not ubiquitous (Benabentos et al., 2009).

The requirement of the engagement of compatible TgrB1 and TgrC1 proteins for cooperative cell movement and cell differentiation in the social amoebae suggests that allorecognition is a prerequisite for entry into the multicellular stage. These crucial aspects of tissue formation have gone unnoticed in social amoebae because most of the previous developmental studies examined homotypic cell populations. Allorecognition might activate one or more pathways to regulate cell behavior either directly or indirectly. Given that minority allotype cells become polarized and engage in coordinated movement within minutes of encountering compatible cells, we speculate that cell motility is directly controlled by substrate-level activation of cytoskeletal regulators. Control of cell differentiation could be directly or indirectly controlled by signaling through TgrB1 and TgC1 and might well involve other signaling pathways. Whatever the mechanisms that control cell movement or differentiation, allorecognition appears to be a ‘gating step’ for the progression of multicellular development.

MATERIALS AND METHODS

Genetic manipulation, growth, and development of *D. discoideum* strain AX4, and its derivatives were carried out as described (Hirose et al., 2011). Uracil (20 µg/ml), G418 (10 µg/ml), Blasticidin S (5 µg/ml) and Hygromycin B (25 µg/ml) were added to HL5 growth media as needed. The strains used in this study are described in Table S4. We cloned the *tgrB1* and *tgrC1* alleles from wild strains by PCR and used a gene replacement approach to introduce them as pairs of matching *tgrB1-tgrC1* alleles by homologous recombination into the resident locus in AX4. We constructed the merodiploid strains by cloning pairs of matching *tgrB1-tgrC1* alleles into the *D. discoideum* expression vector pLPBLP (Faix et al., 2004) and selected for transformants with Blasticidin S. Gene expression was

Development (2015) 142, 3561-3570 doi:10.1242/dev.123281

assessed by quantification of mRNA by RNA-seq as described (Parikh et al., 2010). For chimeric development, we combined multiple strains in defined proportions, as described in the text, at a density of 5×10^6 cells/ml in PDF buffer (20.1 mM KCl, 5.3 mM $MgCl_2{\cdot}6H_20$, 9.2 mM K_2HPO_4, 13.2 mM KH_2PO_4, 0.5 mg/ml streptomycin sulfate, pH 6.4) and deposited an aliquot of 1 ml on a 5-cm non-nutrient agar plate. After 30 min of incubation to allow the cells to settle on the agar surface, excess buffer was absorbed with paper towel, and the agar plates were incubated at room temperature until time of observation.

Promoter-sfGFP constructs

We used superfolder GFP (sfGFP) (Pédelacq et al., 2006) for better responsiveness in promoter activation experiments by adding five to ten codons from the *Dictyostelium* genes in front of the sfGFP start codon to ensure translation of sfGFP (Vervoort et al., 2000). sfGFP gene was amplified by PCR using an sfGFP-F primer with a *Bam*HI recognition site and an sfGFP-R primer adding a *Sal*I site. The resulting amplicon was digested with *Bam*HI and *Sal*I and inserted between *Bam*HI and *Xba*I sites of pcotB/GFP to create pcotB/sfGFP. All promoter-sfGFP fusion constructs in this work were generated from pcotB/sfGFP by excising *cotB* promoter with *Xba*I and *Xho*I and replacing promoters of interest. The other expression constructs used in this study are as follows: pDXA-GFP2 (Levi et al., 2000), pDXA-tdTomato (Hirose et al., 2011), pDXA-tdTomato,hygR (Benabentos et al., 2009), PH-GFP (pWf38) (Dormann et al., 2002), p*cotB*/IGFP (Wang and Kuspa, 2002), pDXA-GFPABD120 (Pang et al., 1998; Washington and Knecht, 2008), RFP-H2b (Fischer et al., 2004).

Time-lapse image acquisition

Development was carried out between glass and agar to minimize spatial complexity in the *z*-axis and for better image resolution. Agar blocks with developing cells were placed upside-down on glass-bottomed dishes (MatTek corporation). Time-lapse images were acquired with a Leica SP50 confocal microscope system.

Quantification of cell migration within population

Positions of GFP and RFP cells were recorded every minute for 5 h after 6 h of starvation. The *xy* coordinates of all labeled cells in each frame were determined using CellProfiler software (Carpenter et al., 2006) and used to calculate the speed (mean displacement±standard error) and the change in their direction of movement (variance of angle) between frames. To minimize the noise of centroid shift coming from cell shape change without moving position, displacement was calculated from $frame_n$ to $frame_{n+3}$ (3-min intervals). Displacement was calculated as the square root of $(x_{n+3}-x_n)^2+(y_{n+3}-y_n)^2$, where x and y are coordinates of centroids of a given cell. Angle change between frames was calculated between two displacement vectors of $frame_n-frame_{n+1}$ and $frame_{n+3}-frame_{n+4}$. The data are described as the variance of all the angle changes. The polarity of cells was assessed by constructing kymographs of GFP boundary fluorescence using QuimP software (Bosgraaf and Van Haastert, 2010). Several trials of each strain combination were analyzed and representative experiments are shown.

Flow cytometry

The test strains co-express RFP under the constitutive actin15 promoter and sfGFP under gene promoters of interest. The test strains were co-developed with non-labeled strains, with compatible or incompatible *tgrB1*/*tgrC1* alleles, on nitrocellulose filter. Developing cells for 10 or 14 h were collected and dissociated to single cells by pipetting. Remaining cell clumps were filtered out by a cell strainer with 40-µm pores. Cells were fixed by 2% paraformaldehyde for 10 min at 22°C, washed once in phosphate buffer, and the cells were analyzed by flow cytometry. The fixed cell population was analyzed with a LSRFortessa Cell Analyzer (BD Biosciences). The test strains were first separated from the unlabeled cells with an RFP-positive gating and subsequently examined for GFP fluorescence.

Chemotaxis assay

The cell mixture (2.5×10^7 cells) containing 1% of AX4-RFP and $tgrB1^{QS31}$/$tgrC1^{QS31}$-GFP was developed on a nitrocellulose filter for 6, 7 or 8 h. Then the cells on the filter were collected in a 50 ml falcon tube and washed once in PDF buffer. Cells were dissociated by vortexing and remaining cell clumps were filtered out with 40 µm cell strainer. The dissociated cell suspension was adjusted to ~2×10^6 cells/ml in PDF buffer, and then placed onto a clean cover glass. The cover glass was placed in a Dunn chemotaxis chamber with a gradient of 0-100 nM cAMP. After waiting 10 min for the cAMP gradient to be formed, images were recorded every 30 s, for 30 min. Trajectories of cells were determined and analyzed using the MTrackJ plugin of ImageJ software (Meijering et al., 2012). The chemotactic index was calculated as the ratio of a cell's displacement towards cAMP to overall displacement of that cell.

Monolayer assay conditions

Cells growing in HL-5 were harvested, then washed and resuspended in spore medium (Serafimidis and Kay, 2005). Cells were placed in a 6-well plate with 5 mM cAMP at 5.0×10^3, 5.0×10^4 and 5.0×10^5 cells/cm^2. Bright-field and green fluorescence images of cells at each density were acquired under identical conditions for comparison.

Transcriptional profile of allorecognition

Five strains with distinct *tgrB1*/*tgrC1* gene pairs were mixed at equal proportions and allowed to co-develop to ensure high levels of non-self encounters (80% initially). Cells were also developed as clonal populations and we mixed their RNAs after development. We collected samples at 4, 8 and 12 h and analyzed mRNA abundances by RNA-seq as described previously (Parikh et al., 2010). We then compared mRNA abundance between the co-developed and the control mixed RNA samples. Using the new version of Bayseq on PIPAx, considering $polyA^+$ genes and normalizing for gene length, we calculated the differential expression of the genes between co-development and mixed RNA samples at each time point. We computed the $\log_2$ of the ratio between the co-development and the mixed samples along with the false discovery rate (FDR) and computed the confidence as $-\log_{10}$(FDR) as described in Table S1. For analyses of differentially regulated genes we selected genes with confidence $\geq$1.0 (FDR$\leq$0.1) and expression differences of greater than twofold [$\log_2$(Codevelopment/RNA mixture) <-1 and $>+1$]. We looked for GO term enrichment of all the differentially expressed genes against the entire Dicty genome as described in Table S3 (The Gene Ontology Consortium, 2015). Statistical analyses were carried out using Matlab (MathWorks).

Competing interests

The authors declare no competing or financial interests.

Author contributions

S.H., G.S. and A.K. designed the experiments; S.H. carried out the experiments; S.H., M.K.-K. and B.S. carried out the RNA-seq and associated analyses; and S.H., G.S. and A.K. wrote the manuscript.

Funding

This work was supported by the National Institutes of Health (NIH) [grant number R01 GM084992]. The flow cytometry and cell sorting core at Baylor College of Medicine is supported by NIH grants [NIAID P30AI036211, NCI P30A125123 and NCRR S10RR024574]. Deposited in PMC for release after 12 months.

Supplementary information

Supplementary information available online at
http://dev.biologists.org/lookup/suppl/doi:10.1242/dev.123281/-/DC1

References

Benabentos, R., Hirose, S., Sucgang, R., Curk, T., Katoh, M., Ostrowski, E. A., Strassmann, J. E., Queller, D. C., Zupan, B., Shaulsky, G. et al. (2009). Polymorphic members of the lag gene family mediate kin discrimination in Dictyostelium. *Curr. Biol.* **19**, 567-572.

Boehm, T. (2006). Quality control in self/nonself discrimination. *Cell* **125**, 845-858.

Bosgraaf, L. and Van Haastert, P. J. M. (2010). Quimp3, an automated pseudopod-tracking algorithm. *Cell Adh. Migr.* **4**, 46-55.

Buss, L. W. (1982). Somatic cell parasitism and the evolution of somatic tissue compatibility. *Proc. Natl. Acad. Sci. USA* **79**, 5337-5341.

Carpenter, A. E., Jones, T. R., Lamprecht, M. R., Clarke, C., Kang, I., Friman, O., Guertin, D. A., Chang, J. H., Lindquist, R. A., Moffat, J. et al. (2006).

CellProfiler: image analysis software for identifying and quantifying cell phenotypes. *Genome Biol.* **7**, R100.
Chen, G., Wang, J., Xu, X., Wu, X., Piao, R. and Siu, C.-H. (2013). TgrC1 mediates cell–cell adhesion by interacting with TgrB1 via mutual IPT/TIG domains during development of Dictyostelium discoideum. *Biochem. J.* **452**, 259-269.
Chen, G., Xu, X., Wu, X., Thomson, A. and Siu, C.-H. (2014). Assembly of the TgrB1–TgrC1 cell adhesion complex during Dictyostelium discoideum development. *Biochem. J.* **459**, 241-249.
Dormann, D., Libotte, T., Weijer, C. J. and Bretschneider, T. (2002). Simultaneous quantification of cell motility and protein-membrane-association using active contours. *Cell Motil. Cytoskel.* **52**, 221-230.
Faix, J., Kreppel, L., Shaulsky, G., Schleicher, M. and Kimmel, A. R. (2004). A rapid and efficient method to generate multiple gene disruptions in Dictyostelium discoideum using a single selectable marker and the Cre-loxP system. *Nucleic Acids Res.* **32**, e143.
Fischer, M., Haase, I., Simmeth, E., Gerisch, G. and Müller-Taubenberger, A. (2004). A brilliant monomeric red fluorescent protein to visualize cytoskeleton dynamics in Dictyostelium. *FEBS Lett.* **577**, 227-232.
Gilbert, O. M., Foster, K. R., Mehdiabadi, N. J., Strassmann, J. E. and Queller, D. C. (2007). High relatedness maintains multicellular cooperation in a social amoeba by controlling cheater mutants. *Proc. Natl. Acad. Sci. USA* **104**, 8913-8917.
Hattori, D., Demir, E., Kim, H. W., Viragh, E., Zipursky, S. L. and Dickson, B. J. (2007). Dscam diversity is essential for neuronal wiring and self-recognition. *Nature* **449**, 223-227.
Hirose, S., Benabentos, R., Ho, H.-I., Kuspa, A. and Shaulsky, G. (2011). Self-recognition in social amoebae is mediated by allelic pairs of tiger genes. *Science* **333**, 467-470.
Ho, H.-I., Hirose, S., Kuspa, A. and Shaulsky, G. (2013). Kin recognition protects cooperators against cheaters. *Curr. Biol.* **23**, 1590-1595.
Hughes, A. L. and Nei, M. (1988). Pattern of nucleotide substitution at major histocompatibility complex class I loci reveals overdominant selection. *Nature* **335**, 167-170.
Iranfar, N., Fuller, D. and Loomis, W. F. (2006). Transcriptional regulation of post-aggregation genes in Dictyostelium by a feed-forward loop involving GBF and LagC. *Dev. Biol.* **290**, 460-469.
Kay, R. R. (1982). cAMP and spore differentiation in Dictyostelium discoideum. *Proc. Natl. Acad. Sci. USA* **79**, 3228-3231.
Kessin, R. H. (2001). *Dictyostelium – Evolution, Cell Biology, and the Development of Multicellularity*. Cambridge, UK: Cambridge University Press.
Kriebel, P. W., Barr, V. A., Rericha, E. C., Zhang, G. and Parent, C. A. (2008). Collective cell migration requires vesicular trafficking for chemoattractant delivery at the trailing edge. *J. Cell Biol.* **183**, 949-961.
Lee, H., Brott, B. K., Kirkby, L. A., Adelson, J. D., Cheng, S., Feller, M. B., Datwani, A. and Shatz, C. J. (2014). Synapse elimination and learning rules co-regulated by MHC class I H2-Db. *Nature* **509**, 195-200.
Levi, S., Polyakov, M. and Egelhoff, T. T. (2000). Green fluorescent protein and epitope tag fusion vectors for Dictyostelium discoideum. *Plasmid* **44**, 231-238.
Mammoto, T., Mammoto, A. and Ingber, D. E. (2013). Mechanobiology and developmental control. *Annu. Rev. Cell Dev. Biol.* **29**, 27-61.
Matthews, B. J., Kim, M. E., Flanagan, J. J., Hattori, D., Clemens, J. C., Zipursky, S. L. and Grueber, W. B. (2007). Dendrite self-avoidance is controlled by Dscam. *Cell* **129**, 593-604.
Mehdiabadi, N. J., Jack, C. N., Farnham, T. T., Platt, T. G., Kalla, S. E., Shaulsky, G., Queller, D. C. and Strassmann, J. E. (2006). Social evolution: kin preference in a social microbe. *Nature* **442**, 881-882.
Meijering, E., Dzyubachyk, O. and Smal, I. (2012). Methods for cell and particle tracking. *Methods Enzymol.* **504**, 183-200.
Ostrowski, E. A., Katoh, M., Shaulsky, G., Queller, D. C., Strassmann, J. E. and Barton, N. H. (2008). Kin discrimination increases with genetic distance in a social amoeba. *PLoS Biol.* **6**, e287.
Pang, K. M., Lee, E. and Knecht, D. A. (1998). Use of a fusion protein between GFP and an actin-binding domain to visualize transient filamentous-actin structures. *Curr. Biol.* **8**, 405-408.
Parent, C. A., Blacklock, B. J., Froehlich, W. M., Murphy, D. B. and Devreotes, P. N. (1998). G protein signaling events are activated at the leading edge of chemotactic cells. *Cell* **95**, 81-91.
Parikh, A., Miranda, E. R., Katoh-Kurasawa, M., Fuller, D., Rot, G., Zagar, L., Curk, T., Sucgang, R., Chen, R., Zupan, B. et al. (2010). Conserved developmental transcriptomes in evolutionarily divergent species. *Genome Biol.* **11**, R35.
Pédelacq, J.-D., Cabantous, S., Tran, T., Terwilliger, T. C. and Waldo, G. S. (2006). Engineering and characterization of a superfolder green fluorescent protein. *Nat. Biotechnol.* **24**, 79-88.
Rappel, W.-J., Nicol, A., Sarkissian, A., Levine, H. and Loomis, W. F. (1999). Self-organized vortex state in two-dimensional Dictyostelium dynamics. *Phys. Rev. Lett.* **83**, 1247-1250.
Rietdorf, J., Siegert, F. and Weijer, C. J. (1996). Analysis of optical density wave propagation and cell movement during mound formation in Dictyostelium discoideum. *Dev. Biol.* **177**, 427-438.
Rosa, S. F. P., Powell, A. E., Rosengarten, R. D., Nicotra, M. L., Moreno, M. A., Grimwood, J., Lakkis, F. G., Dellaporta, S. L. and Buss, L. W. (2010). Hydractinia allodeterminant alr1 resides in an immunoglobulin superfamily-like gene complex. *Curr. Biol.* **20**, 1122-1127.
Saxe, C. L., III, Ginsburg, G. T., Louis, J. M., Johnson, R., Devreotes, P. N. and Kimmel, A. R. (1993). CAR2, a prestalk cAMP receptor required for normal tip formation and late development of Dictyostelium discoideum. *Genes Dev.* **7**, 262-272.
Serafimidis, I. and Kay, R. R. (2005). New prestalk and prespore inducing signals in Dictyostelium. *Dev. Biol.* **282**, 432-441.
Sukumaran, S., Brown, J. M., Firtel, R. A. and McNally, J. G. (1998). lagC-null and gbf-null cells define key steps in the morphogenesis of Dictyostelium mounds. *Dev. Biol.* **200**, 16-26.
The Gene Ontology Consortium (2015). Gene Ontology Consortium: going forward. *Nucleic Acids Res.* **43**, D1049-D1056.
Thompson, C. R. L. and Kay, R. R. (2000). Cell-fate choice in Dictyostelium: intrinsic biases modulate sensitivity to DIF signaling. *Dev. Biol.* **227**, 56-64.
Tomchik, K. J. and Devreotes, P. N. (1981). Adenosine 3′,5′-monophosphate waves in Dictyostelium discoideum: a demonstration by isotope dilution–fluorography. *Science* **212**, 443-446.
Umeda, T. and Inouye, K. (2002). Possible role of contact following in the generation of coherent motion of Dictyostelium cells. *J. Theor. Biol.* **219**, 301-308.
Vervoort, E. B., van Ravestein, A., van Peij, N. N. M. E., Heikoop, J. C., van Haastert, P. J. M., Verheijden, G. F. and Linskens, M. H. K. (2000). Optimizing heterologous expression in dictyostelium: importance of 5′ codon adaptation. *Nucleic Acids Res.* **28**, 2069-2074.
Wang, B. and Kuspa, A. (1997). Dictyostelium development in the absence of cAMP. *Science* **277**, 251-254.
Wang, B. and Kuspa, A. (2002). CulB, a putative ubiquitin ligase subunit, regulates prestalk cell differentiation and morphogenesis in Dictyostelium spp. *Eukaryot. Cell* **1**, 126-136.
Wang, J., Hou, L., Awrey, D., Loomis, W. F., Firtel, R. A. and Siu, C.-H. (2000). The membrane glycoprotein gp150 is encoded by the lagC gene and mediates cell–cell adhesion by heterophilic binding during Dictyostelium development. *Dev. Biol.* **227**, 734-745.
Washington, R. W. and Knecht, D. A. (2008). Actin binding domains direct actin-binding proteins to different cytoskeletal locations. *BMC Cell Biol.* **9**, 10.
Weijer, C. J. (2009). Collective cell migration in development. *J. Cell Sci.* **122**, 3215-3223.
Williams, J. (1997). Prestalk and stalk heterogeneity in Dictyostelium. In *Dictyostelium – A Model System for Cell and Developmental Biology* (ed. Y. Maeda, K. Inouye and I. Takeuchi), pp. 293-304. Tokyo, Japan: Universal Academy Press.
Zhang, L. and Wrana, J. L. (2014). The emerging role of exosomes in Wnt secretion and transport. *Curr. Opin. Genet. Dev.* **27**, 14-19.